# Modeling the Effects of Surface Recombination Velocity in Scanning Photocurrent Microscopy for Ohmic-Contact Thin-Film Devices

Yu-Chien Wei[1,*] and Ming-Hua Mao[1,2,3]

[1]Graduate Institute of Electronics Engineering, [2]Department of Electrical Engineering, [3]Graduate Institute of Photonics and Optoelectronics, National Taiwan University, Taipei 10617, Taiwan
*Yu-Chien Wei: f07941001@ntu.edu.tw

*Abstract-* **We studied numerically the carrier transport and confirmed the feasibility of our scanning photocurrent microscopy model in the minority carrier decay length extraction under different surface recombination velocities at the surfaces of ohmic-contact thin-film devices.**

## I. Introduction

Understanding of the carrier transport behavior and other material properties is important in development of nano-scaled semiconductor devices. Scanning photocurrent microscopy (SPCM) has been used to extract the minority carrier decay length in both one-dimensional (1D) [1] and two-dimensional (2D) [2] transport structures. The schematic of SPCM is shown as Fig. 1(a). The etching process in the fabrication of thin-film devices as we previously reported [2] would lead to the increase of surface recombination velocity S which influences the carrier transport property. In this paper, we studied the carrier transport and confirmed the feasibility of the SPCM model in the minority carrier decay length extraction [2] under different surface recombination velocities at the surface of thin-film sidewalls by Synopsys Sentaurus Technology Computer Aided Design (TCAD) simulations.

## II. TCAD Simulation Methodology

Here, we used a n-type InAs thin film in TCAD simulations with a three-dimensional (3D) model. The device channel between two electrodes is 1 μm in width, 5 μm in length, and 0.2 μm in thickness. The coordinates are defined in Fig. 1(a) with the origin at the center of the thin film channel. The laser source was incident on the top surface and scanned across the channel along $(y, z) = (0.0, 0.1)$ μm. Its 2D Gaussian shape was utilized as the absorbed photon density profile and the spot size was 100 nm. The absorbed photon density per second was calculated from the laser pumping power and 100% conversion of absorbed photons into electron-hole pairs was assumed. The absorbed photon density per second has a peak value of $8 \times 10^{23}$ $cm^{-3} \cdot s^{-1}$, corresponding to the laser pumping density of about 20 W·cm$^{-2}$. For the case of n-type InAs thin film, both material parameters of InAs and the operation setting in simulations are the same as those used in our previous work [2] except the additional model of the surface recombination velocity in this study. The typical drift-diffusion transport framework along with the Shockley-Read-Hall recombination model, Auger recombination model, and the constant mobility model was considered. The material parameters are shown below: net doping $N_D$ $10^{17}$ cm$^{-3}$, minority carrier lifetime τ 660 ps [1], electron mobility $\mu_n$ 4000 cm$^2 \cdot V^{-1} \cdot s^{-1}$ [3], hole mobility $\mu_p$ 60

cm$^2 \cdot V^{-1} \cdot s^{-1}$ [4], and Auger coefficient of $2.2 \times 10{-}27$ cm$^6 \cdot s^{-1}$ [5]. The bias of 0.01 V is set on the anode of the device, which corresponds to an applied electric field of 20 V·cm$^{-1}$.
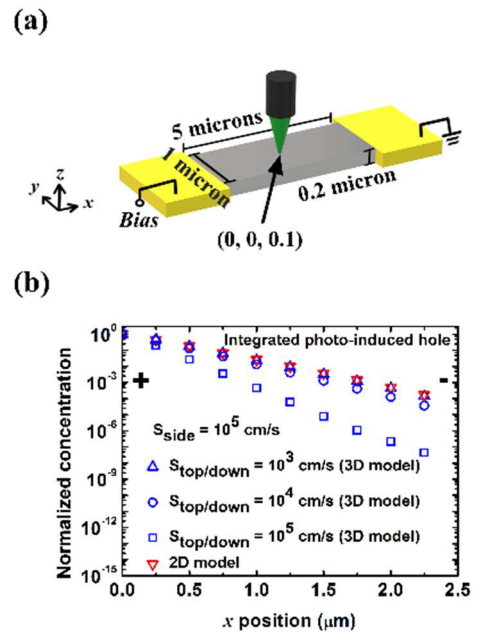


Fig. 1. (a) Schematic of a SPCM setup in a two-terminal thin-film structure. (b) Integrated photo-induced hole distributions of the 3D/2D model. $S_{side}$ is fixed at $10^5$ cm/s.

## III. Results and Discussions

The y- and z-direction-integrated photo-induced hole distributions under laser excitation at the center of the top surface $(x, y, z) = (0.0, 0.0, 0.1)$ μm with different surface recombination velocities at top/down surface $S_{top/down}$ are shown in Fig. 1(b), where the surface recombination velocity at the sidewall surface $S_{side}$ is fixed at $10^5$ cm/s. It has been indicated that the integrated photo-induced carrier distribution can be appropriately described by the 1D drift-diffusion model [2]. We also simulated the hole distribution with a 2D model and the fixed value of $S_{side} = 10^5$ cm/s. In Fig. 1(b), with decreasing $S_{top/down}$ from $10^5$ cm/s to $10^4$ cm/s, carrier decay length in a 3D model becomes significantly longer. With $S_{top/down} = 10^3$ cm/s, carrier decay length in a 3D model almost matches that in a 2D model, where $S_{top/down}$ is two orders of magnitudes smaller than $S_{side}$. As demonstrated in our previous work [2], a dry etching process was used in our device fabrication. Due to the ion damaging on the exposed surface of

141

the sidewall during the dry etching process, we believe that the $S_{side}$ is much higher than the $S_{top/down}$ in our device. Hence, we can use the 2D model with only specified $S_{side}$ in the following study instead of the 3D model with various $S_{top/down}$ and $S_{side}$ in our simulation.

Fig. 2(a) shows the result of the *y*-direction-integrated photo-induced hole distribution with different $S_{side}$ under laser excitation at the center of the surface (x, y) = (0, 0), using the 2D model. From the fitted decay length of the integrated photo-induced hole distribution, we can calculate the carrier lifetime by the drift-diffusion model in combination with Einstein relation. The calculated carrier lifetime with different $S_{side}$ is plotted in Fig. 2(b). Our results are in agreement with those of the analytical approximation in the high/low surface recombination velocity condition [6] plotted as the dashed line.
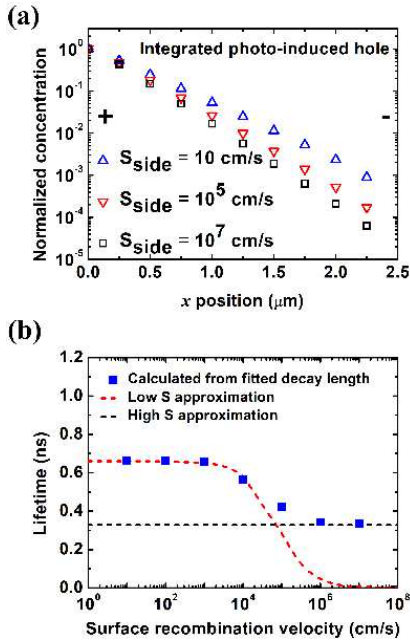


Fig. 2. (a) Integrated photo-induced hole distribution of the 2D model with different $S_{side}$. (b) Calculated carrier lifetime under different $S_{side}$. Dashed lines represent the analytical approximation in the high/low surface recombination velocity condition.

Finally, we simulated the scanning photocurrent profiles on the cathode side with different $S_{side}$ as shown in Fig. 3(a). We can extract the minority carrier decay length by fitting these photocurrent profiles with the analytic formula of our SPCM model [2]

$$a - be^{x/L_{fit}} \tag{1}$$

where the symbols a and b are the fitting parameters. And the fitted decay length $L_{fit}$ corresponds to minority carrier (hole) decay length for cathode region, which must be a positive number. With different $S_{side}$, the fitted decay length extracted from the scanning photocurrent profile is almost the same as that from the integrated photo-induced hole distribution. This shows the feasibility of our SPCM model in the minority carrier decay length extraction under different surface recombination velocities.

## IV. CONCLUSION

In this paper, we numerically studied the carrier transport using SPCM under different surface recombination velocities at the surface of thin-film devices. The simulation result

showed that we can use the 2D model with only specified $S_{side}$ in our study instead of the 3D model with various $S_{top/down}$ and $S_{side}$, since $S_{side}$ is typically two orders of magnitude larger than $S_{top/down}$ due to the ion-damaged sidewalls induced by the dry etching process. Then we also confirmed that the calculated carrier lifetimes of the device under different surface recombination velocity conditions are in agreement with those of the analytical approximation in the literature. Finally, we simulated the scanning photocurrent profiles and showed the feasibility of our SPCM model in the minority carrier decay length extraction under different surface recombination velocities.
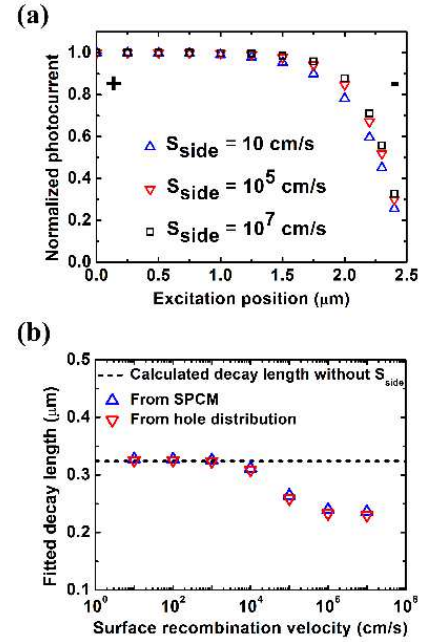


Fig. 3. (a) Scanning photocurrent profiles of the 2D model with different $S_{side}$. (b) The fitted decay length extracted from both scanning photocurrent profiles and the integrated photo-induced hole distribution under different $S_{side}$.

## REFERENCES

[1] C. H. Chu, M.-H. Mao, C. W. Yang & H. H. Lin, "A New Analytic Formula for Minority Carrier Decay Length Extraction from Scanning Photocurrent Profiles in Ohmic-Contact Nanowire Devices," Sci. Rep 9 (2019).

[2] Y. C. Wei, C. H. Chu & M.-H. Mao, "Minority carrier decay length extraction from scanning photocurrent profiles in two-dimensional carrier transport structures," Sci. Rep 11, 21863 (2021).

[3] Takita, H. et al. Electron transport properties of InAs ultrathin films obtained by epitaxial lift-off and van der Waals bonding on flexible substrates. Appl. Phys. Lett. 97, 3 (2010).

[4] Sotoodeh, M., Khalid, A. H. & Rezazadeh, A. A. Empirical low-field mobility model for III-V compounds applicable in device simulation codes. J. Appl. Phys. 87, 2890-2900 (2000).

[5] Mikhailova, M. P. Levinshtein, M., Rumyantsev, S. & Shur, M. (ed.) Handbook Series on Semiconductor Parameters. Chapter 7, 159 (World Scientific, 1996).

[6] R. K. Ahrenkiel, "In Semiconductors and Semimetals" Vol. 39 39–150 (1993).